2026 IEEE/SICE International Symposium on System Integration (SII)
January 11-14, 2026. Cancún, México

Three-dimensional Knee Joint Load Estimation System During Walking Using IMU Sensors for the Prevention of Knee Osteoarthritis: A Fundamental Study

R. Yoshizawa, A. Uehara*, Y. Sankai, and H. Kawamoto

Abstract— **Knee osteoarthritis (KOA) is a serious disease affecting one-third of the world's population, and mechanical loading on the knee joint has been identified as a progressive factor. However, conventional knee contact force measurements are limited to laboratory environments, making daily preventive monitoring difficult. This fundamental study aims to establish the optimal deep learning approach for three-dimensional knee contact force estimation using wearable IMU sensors and to validate the technical feasibility for practical KOA prevention systems. Methodologically, four deep learning models were systematically compared: 1D-CNN, LSTM, RNN, and Transformer. These models were trained to map 45-channel IMU time-series data comprising three-axis acceleration, angular velocity, and magnetic field from five anatomical locations to six-dimensional knee contact forces through 7-fold cross-validation. The 1D-CNN achieved the optimal maximum error of 24.01 %, while LSTM demonstrated the most stable average error of 13.93 %. These results showed superior performance compared to existing IMU-based methods, realizing three-dimensional knee joint force estimation within the practical accuracy range of wearable healthcare devices. This fundamental study successfully established the technical feasibility of translating laboratory-based knee joint load assessment to daily environments and presented clear guidelines for developing non-invasive KOA prevention systems.**

I. Introduction

Knee osteoarthritis (KOA) is the most common degenerative joint disease. Epidemiological studies indicate that approximately one-third of the global population aged more than 50 years is affected, with one in six experiencing symptomatic pain[1]. Individuals with KOA face increased risks of limited physical function, greater need for long-term care, and significant reductions in their quality of life and independence[2]. This vulnerability in older adults stems from age-related joint degeneration, decreased cartilage repair capabilities, and the cumulative effects of joint injuries over a lifetime, all of which contribute to the increased risk of KOA with aging[3]. Furthermore, since scientific evidence has demonstrated that excessive mechanical loading of the knee joint accelerates KOA progression[4], continuous monitoring of knee contact forces during daily activities and early appropriate preventive intervention represent the key to KOA countermeasures in an aging society. However, currently available knee joint load measurement technologies are limited to laboratory environments, presenting a significant technical challenge for their application to daily preventive care.

Methods for measuring knee joint loads include the use of pressure sensors embedded in knee implants[5][6]. However, these approaches require highly invasive surgical procedures, limiting their applicability in healthy individuals and older adults. Noninvasive measurement approaches typically involve simulations using musculoskeletal modeling software, such as OpenSim[7] or AnyBody[8]. OpenSim enables the noninvasive estimation of knee contact forces, including interbone contact forces, ligament and joint capsule tensions, muscle forces, external loads, and inertial forces. However, this method requires three-dimensional positional data from optical motion capture systems and force information from force plates as inputs. These measurement devices are environment-dependent, rendering them unsuitable for continuous monitoring of knee joint loads during daily activities. Recent advances in deep learning for time-series biosignal processing have reported significant achievements in areas including motion classification, ground reaction force estimation, and gait feature extraction and anomaly detection. Research has progressed toward estimating ground reaction forces and joint angles using multiple small, lightweight inertial measurement units (IMUs) worn during daily activities to assess knee joint loads[9][10]. Additionally, studies have estimated the first and second peaks of knee contact forces using fully connected neural networks trained on IMU data collected from the waist, thigh, and lower legs as inputs[11]. These technological advances have made technology transfer from laboratory to daily environments realistic, establishing the foundation for continuous healthcare systems. However, existing research on IMU-based knee contact force estimation has the following technical limitations: first, primary focus on one-dimensional estimation emphasizing sagittal plane flexion-extension movements; second, lack of comprehensive measurement and evaluation of three-dimensional knee joint loads necessary for KOA prevention; third, insufficient systematic comparison of various deep learning models in time-series data processing.

This study includes the results of Cross-ministerial Strategic Innovation Promotion Program (SIP) 3rd Phase, ”Expansion of fundamental technologies and development of rules promoting social implementation to expand HCPS Human-Collaborative Robotics” promoted by Council for Science, Technology and Innovation(CSTI), Cabinet Office, Government of Japan. (Project Management Agency: New Energy and Industrial Technology Development Organization (NEDO), Project Code: JPJ012494, HCPS: Human-Cyber-Physical Space)

R. Yoshizawa is with the Graduate School of Science and Technology, University of Tsukuba, Ibaraki, Japan.
(e-mail: yoshizwa@golem.iit.tsukuba.ac.jp).

A. Uehara, Y. Sankai and H. Kawamoto are with the Institute of Systems and Information Engineering, Center for Cybernics Research, University of Tsukuba, Tsukuba, Ibaraki,Japan
(e-mail: {uehara, sankai, kawamoto}@golem.iit.tsukuba.ac.jp)..

To address these limitations and realize practical KOA prevention systems for daily use, this fundamental study aims to establish the optimal deep learning approach for three-dimensional knee contact force estimation using wearable IMU sensors. The specific objectives are threefold: first, to systematically compare four representative deep learning models for mapping multivariate IMU time-series data to three-dimensional knee contact forces; second, to identify the optimal architecture balancing accuracy and stability for continuous healthcare monitoring; third, to validate the technical feasibility and establish performance benchmarks for translating laboratory-based knee joint load assessment to daily environments. This fundamental study serves as a critical foundation for developing non-invasive KOA prevention systems that enable early intervention and personalized healthcare management in aging societies.

II. Materials And Methods

A. Dataset

To evaluate the effectiveness of the developed system, gait data from a healthy adult male participant were collected. The experiment was conducted in compliance with the ethical principles of the Declaration of Helsinki by the World Medical Association, and informed consent was obtained from the participant based on free will prior to participation in the research. The participant was instructed to walk at a self-selected comfortable speed, performing 15 trials of straight-line walking crossing force plates in four steps. Trials lacking proper time synchronization or unsuitable for OpenSim analysis were excluded from the collected data, yielding seven valid datasets for model training and evaluation.

Each gait trial was recorded at a sampling frequency of 100 Hz. A single dataset contained approximately 100-150 time frames corresponding to one complete gait cycle, yielding a total of approximately 700-1050 frames across all seven datasets. After applying the sliding window approach with 81-frame windows and one-frame step size, each dataset generated approximately 20-70 training samples, resulting in approximately 140-490 total training samples across all datasets. Within each trial, time segments where foot contact with force plates was confirmed were selected for analysis. For evaluation metric calculations, only stance phases identified from force plate data were used, as knee contact forces during swing phases are minimal and of limited clinical significance.

B. IMU Sensing System

Figure 1 illustrates the overall system architecture for three-dimensional knee contact force estimation. The system integrates wearable IMU sensors positioned at multiple anatomical locations with deep learning models to estimate knee joint loads in real-time. The workflow demonstrates how raw IMU sensor data are processed through preprocessing stages and fed into machine learning models to predict three-dimensional knee contact forces that would traditionally require laboratory-based motion capture and force plate systems. Specifically, the neural network models map 45-dimensional input vectors $\mathbf{x}$ comprising three-axis acceleration, angular velocity, and magnetic field measurements from five IMU sensors to 6-dimensional output vectors y representing three-dimensional knee contact forces for both left and right knees, mathematically expressed as $\mathbf{y} = f(\mathbf{x})$, where f represents the learned nonlinear mapping function implemented by each deep learning architecture.

Miniaturization and weight reduction of IMU sensing systems are essential for enabling continuous sensing during daily activities. In this study, high-precision IMU sensor modules developed by our research group were employed[12]. These modules enable accurate measurement of a wide range of movements from low to high speeds by integrating two types of sensors with different measurement ranges. The sensor modules operate at a sampling frequency of 1 kHz and incorporate a three-axis accelerometer, a three-axis gyroscope, and a three-axis magnetometer. For the present study, the IMU sensing system consisted of five IMU sensor modules and a host PC, allowing for the detailed capture of motion data during walking.

C. Data Collection Protocol

The data required to construct the three-dimensional knee contact force estimation model were collected simultaneously using the IMU sensing system, optical motion-capture system, and force plates. As shown in Figure 2, the IMU sensor modules were positioned at anatomically

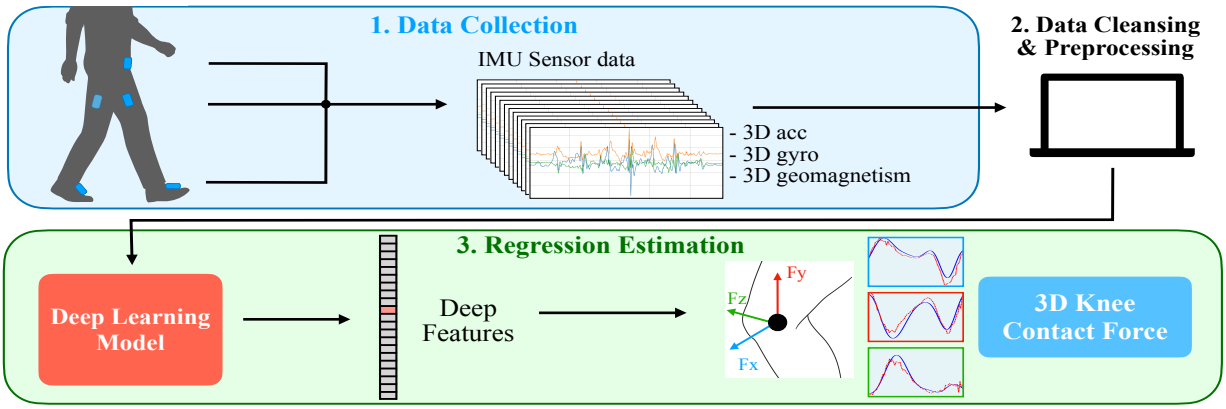

Figure 1. Overview of the three-dimensional knee contact force estimation system.

significant locations: one on the lower abdomen, two on the lateral aspects of both thighs, and two on the dorsal surfaces of both feet, to measure acceleration, angular velocity, and magnetic field. For optical motion capture, a VICON MX system consisting of 16 cameras was used to record three-dimensional position data at a sampling frequency of 100 Hz. The Plug-in Gait marker set[13], which is compatible with OpenSim data inputs, was employed. Ground reaction forces were measured using OR6 series force plates, which recorded three-dimensional ground reaction forces acting on both feet at a sampling frequency of 1 kHz. These measurements enabled the construction of a multifaceted walking dataset. Figure 3 presents a depiction of the experimental procedure alongside the corresponding OpenSim simulation.

D. Knee Contact Force Estimation Based on the Musculoskeletal Model

A sixth-order low-pass filter was applied to the marker and ground reaction force data, and musculoskeletal

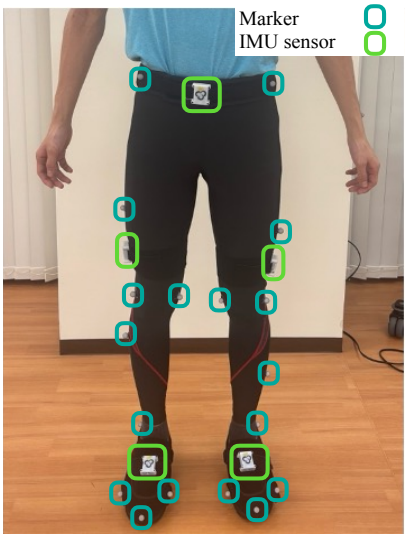

Figure 2. Front view of the measurement setup, showing the placement of IMU sensor modules and markers used in the optical motion capture system.

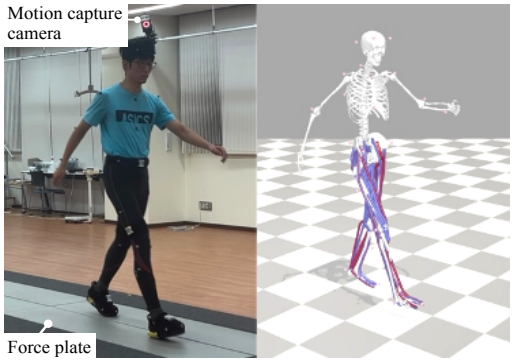

Figure 3. Representative image of the experimental measurement setup and the corresponding musculoskeletal model-based estimation using OpenSim.

modeling was performed using the OpenSim model Catelli_high_hip_Flexion_V4.0[14]. The model was scaled according to the marker positions in a static posture to match the anthropometric measurements of the participants. Subsequently, joint angles were calculated using OpenSim's Inverse Kinematics Tool, and the tension in the lower limb muscle groups was computed using the Static Optimization Tool. Finally, knee contact forces were calculated as three-dimensional vectors representing the force exerted on the tibia relative to the femur across the entire walking data, using the Joint Reaction Force Analysis Tool. This process yielded high-precision knee contact force data that served as the ground truth for the machine learning model.

E. Preprocessing and Data Cleansing

Outlier processing was applied to the angular velocity data acquired from the IMU sensors by excluding values with z-scores greater than three, followed by linear interpolation. For the magnetic field data, soft- and hard-iron corrections were performed based on the indoor magnetic field distribution data measured using a nonmagnetic resin gimbal that did not affect the geomagnetic field. Equation (1) describes the formula used for soft- and hard-iron correction.

$$\boldsymbol{m}_{\mathrm{c}} = \boldsymbol{S}(\boldsymbol{m}_{\mathrm{raw}} - \boldsymbol{h}) \quad (1)$$

where $\boldsymbol{m}_{\mathrm{c}}$ is the corrected value of the magnetic field vector, $\boldsymbol{m}_{\mathrm{raw}}$ is the measured value of the magnetic field vector, $\boldsymbol{S}$ is the soft-iron correction matrix that restores the magnetic field vector distribution to an ideal spherical distribution, and $\boldsymbol{h}$ is the hard-iron offset vector. Additionally, noise in the knee contact force data was reduced using a fourth-order zero-phase Butterworth filter with a 6 Hz cutoff frequency.

To align the timestamps of data calculated using OpenSim with those acquired from the IMU sensor modules, missing timestamp data were interpolated using spline interpolation and expanded to a sampling rate of 1 kHz, then downsampled to 100 Hz. The IMU and knee contact force data were scaled to minimize loss during machine learning. The acceleration, angular velocity, and magnetic field data were clipped to ranges of ± 5 G, ± 500 °/s, and ± 5 μT, respectively, applied to each x, y, and z component of the sensors. Because the knee contact force components differed significantly in magnitude across the axes, they were normalized using axis-specific scaling factors: the value x was divided by 500, value y by 4500, and value z by 1000. A synchronization signal was recorded using a manual switch at the start of the walking motion measurement. Synchronization processing was performed between the data acquired by IMU sensor modules, knee contact forces calculated using OpenSim, and ground reaction force data from force plates by aligning their start times to the recorded synchronization signal.

F. Construction of Three-Dimensional Knee Joint Contact Force Estimation Model

In tthis study, four representative deep learning architectures were implemented with the aim of identifying the optimal approach for time-series knee joint contact force estimation. The training data were structured as

time-synchronized sequences, aligning IMU sensor data from five anatomical locations to the corresponding three-dimensional knee contact force data for both legs estimated using OpenSim. The input data **x** comprised 45 channels: three-axis acceleration, three-axis angular velocity, and three-axis magnetic field from each of the five sensors. The output data **y** comprised 6 channels: three-dimensional forces for both left and right knees. Window processing was applied to each sequence data by sliding a time window of 81 frames forward by one frame at a time. Each deep learning model learned the nonlinear mapping function f such that $\mathbf{y} = f(\mathbf{x})$, where the specific implementation of f differed according to the architectural characteristics of each model.

1D-CNN[15][16]: This architecture employed hierarchical feature extraction through multiscale convolutional operations. The network processed input sequences $\mathbf{x} \in \mathbb{R}^{T\times 45}$ where T represents the temporal dimension. Initial convolution layers with kernel sizes of 1, 3, 5, and 7 operated in parallel to extract features at multiple temporal scales, followed by concatenation and fusion through subsequent convolutional layers. Skip connections were introduced to address vanishing gradients, with Batch Normalization and GELU activation functions applied after each layer. The final layer compressed the feature representation to produce output $\mathbf{y} \in \mathbb{R}^{T\times 6}$ corresponding to six-dimensional knee contact forces.

LSTM[17]: The network architecture comprised an input projection layer, bidirectional LSTM layers with 128 hidden units, and attention mechanisms. The model processed sequential input $\mathbf{x}_t$ at each time step t, maintaining hidden states $\mathbf{h}_t$ and cell states $\mathbf{c}_t$ to capture long-term dependencies through gate mechanisms: forget gate, input gate, and output gate. Dropout regularization of 0.2 was applied to prevent overfitting. The final output layer mapped the learned temporal representations to six-dimensional knee contact forces while preserving sequential information.

RNN[18]: A basic recurrent architecture with 128 hidden units was implemented as a baseline model. The network propagated information through hidden states $\mathbf{h}_t = \tanh(\mathbf{W}_{xh}\,\mathbf{x}_t + \mathbf{W}_{hh}\,\mathbf{h}_{t-1} + \mathbf{b}_h)$, where $\mathbf{W}_{xh}$ and $\mathbf{W}_{hh}$ represent weight matrices and $\mathbf{b}_h$ represents bias terms. This simplified architecture enabled direct comparison with LSTM to evaluate the impact of vanishing gradient problems in knee contact force estimation.

Transformer[19]: This architecture employed self-attention mechanisms to capture long-range dependencies in parallel. Input sequences were first projected to 128-dimensional embeddings and combined with positional encodings to preserve temporal information. Multi-head attention with 8 heads computed attention weights across all time steps, enabling the model to focus on relevant temporal patterns. Layer normalization and feed-forward networks were applied in each transformer block to produce the final six-dimensional force predictions.

G. Model Evaluation Metrics

During model training, the mean squared error (MSE) was adopted as the loss function to minimize the discrepancy between the estimated and measured values (Equation 2).

$$MSE = \frac{\sum_{t=1}^{N}(\tilde{y}_t - \mathrm{y}_t)^2}{N} \tag{2}$$

Where $\tilde{y}_t$ denotes the predicted value, y_t is the measured value, and N is the number of frames.

To uniformly evaluate the estimation performance of each model, the normalized root mean square error (NRMSE) of the knee contact force in the test data was used (Equation 3).

$$NRMSE = \frac{\sqrt{\frac{\sum_{t=1}^{N}(\tilde{y}_t - y\theta_t)^2}{N}}}{\tilde{y}_{\max} - \tilde{y}_{\min}} \tag{3}$$

where $\tilde{y}_{\max}$ and $\tilde{y}_{\min}$ represent the maximum and minimum measured values, respectively. NRMSE is an error indicator normalized by the range of values, facilitating comparison between different components and other research. For the calculated NRMSE, comprehensive comparison of mean values, standard deviations, minimum and maximum values across all folds, and component-specific detailed analysis were performed to identify important indicators for preventive system design.

For data cross-validation methodology, 7-fold nested cross-validation was executed. Specifically, in the outer loop, one of the seven datasets was designated as the test set, with the remaining six used for training and validation. In the inner loop, the six training and validation datasets were further utilized for hyperparameter optimization. In the outer loop, ensemble averages of six trained models were applied to test data to evaluate the accuracy of final estimation.

III. Results

A. Model Performance Comparison

To comprehensively evaluate the performance of each deep learning model, two types of comparative analyses were conducted. Table 1 presents the overall performance comparison across all models using statistical measures of NRMSE, including mean, maximum, minimum, and standard deviation values calculated from 7-fold cross-validation results. This table provides insights into both the average accuracy and stability of each model for practical healthcare applications. Table 2 provides a detailed breakdown of the maximum NRMSE values for each knee joint force component Fx, Fy, Fz across both left and right knees. This component-wise analysis is crucial for identifying which specific force directions present the greatest estimation challenges and require particular attention in preventive healthcare monitoring systems. Figure 4 shows the performance comparison results of each deep learning model for knee joint contact force estimation.

Table 1. Summary statistics of NRMSE for knee contact force estimation across all components and models (%)

Model	Mean	Max	Min	Std
LSTM	13.93	24.47	6.48	4.87
1D-CNN	14.50	24.01	6.38	4.91
RNN	18.24	27.56	9.70	3.83
Transformer	17.91	26.97	10.85	3.48

Table 2. Maximum normalized root means square error (NRMSE) values across different deep learning architectures for estimating knee contact force components in the Fx, Fy, and Fz directions Error Analysis : Maximum NRMSE (%)

Component	1D-CNN	LSTM	RNN	Transformer
L Knee Fx	18.65	19.8	19.39	20.12
L Knee Fy	24.01	24.47	27.56	24.74
L Knee Fz	23.9	20.61	22.8	23.11
R Knee Fx	13.09	15.89	23.67	21.39
R Knee Fy	20.59	21.86	26.88	26.97
R Knee Fz	23.22	19.58	20.51	21.13

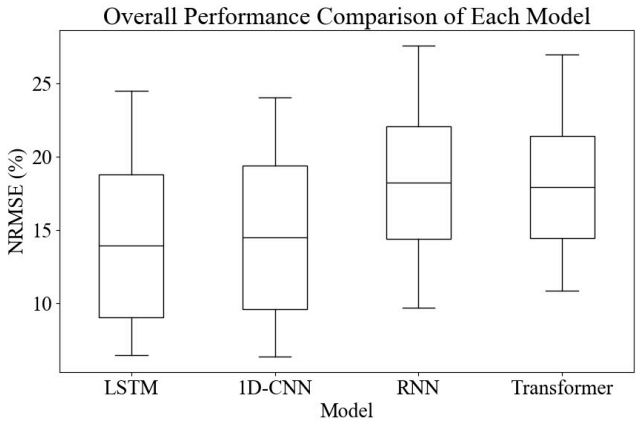

Figure 4. NRMSE distribution comparison across ML models for knee joint force prediction. Box plots show performance variability for 1D-CNN, LSTM, RNN, and Self-Attention models across all joint components and cross-validation folds.

B. Detailed Analysis Results

Best Performance Model (Mean NRMSE Criteria):
LSTM: 13.93 % - Optimal stable estimation accuracy for long-term health status tracking
1D-CNN: 14.50 % - Good performance following LSTM
Important Indicators for Continuous Healthcare Applications (Maximum NRMSE Criteria):
1D-CNN: 24.01 % - Optimal maximum error level for daily monitoring
LSTM: 24.47% - Prevention system applicability following 1D-CNN
Most Challenging Estimation Component:
All models showed maximum errors in the left knee Fy component (24.01-27.56 %), revealing that this component is a particularly important indicator requiring attention in OA prevention. RNN recorded the highest error of 27.56 %, clearly demonstrating the limitations of basic recurrent structures.

IV. Discussion

The maximum error of 24.01 % achieved by 1D-CNN in the proposed system was lower than the estimation error of 26.6 ± 7.5 % reported in previous studies using multiple IMU sensors[11]. In this fundamental study, by extending conventional one-dimensional estimation to complete three-dimensional estimation including anterior-posterior and medial-lateral components, we achieved technical advances essential for comprehensive preventive evaluation of KOA. Through systematic performance comparison of four deep learning models, 1D-CNN showed the best performance with the most important maximum error for continuous healthcare monitoring, while LSTM demonstrated the most stable performance with average error. The conventional RNN method showed the highest maximum error of 27.56 %, clearly revealing the impact of vanishing gradient problems in knee contact force estimation. The Transformer model also did not show significant superiority compared to other deep learning methods, suggesting that the characteristics of knee contact force data are more suitable for convolutional and gate mechanisms than attention mechanisms.

The superiority of 1D-CNN is attributed to local feature extraction by convolutional layers being suitable for capturing instantaneous variation patterns of knee contact forces. In daily KOA prevention systems, detecting changes in load patterns through continuous monitoring is important, and the accuracy level achieved in this fundamental study has the following preventive medical value: first, abnormal pattern detection capability where even with 24.01 % accuracy, detection of significant increases in knee joint loads and abnormal patterns is sufficiently possible; second, long-term trend monitoring where early warning of KOA progression risk is realized through tracking relative changes in daily activities; third, personalized healthcare where personalized preventive guidance becomes possible through monitoring intra-individual changes after baseline establishment. Furthermore, the observation that all models showed maximum errors in the left knee Fy component suggests that loads in this direction are particularly important indicators requiring attention in KOA progression, and implementation of focused monitoring algorithms would be effective in prevention systems. The component-specific error variations observed across different force directions may be influenced by several factors including gait habits, sensor placement accuracy, and inherent biomechanical characteristics of knee joint loading patterns. However, the consistent identification of the Fy component as the most challenging across all models suggests this represents a fundamental characteristic of knee joint force estimation rather than random experimental variation. As accuracy standards for wearable healthcare devices, estimation errors of 20-30 % are considered practical ranges for non-invasive biomechanical analysis devices, and this fundamental study's 24.01 % demonstrates excellent performance within this standard. The consistent performance level demonstrated through 7-fold cross-validation indicates statistical reliability and meets reproducibility requirements for continuous healthcare applications.

This fundamental study has the following limitations. First, evaluation with a single subject without consideration of individual differences and body type variations limits generalizability. The limited dataset size may particularly affect the performance of complex models such as Transformer, which typically require larger training datasets to fully leverage their capacity for learning long-range dependencies. Second, real-time processing performance

evaluation was not conducted, with insufficient assessment of computational load and power consumption in actual daily use. Third, non-uniformity in component-specific accuracy exists, with all models showing maximum errors particularly in the left knee Fy component. Fourth, while the achieved accuracy level is suitable for daily preventive and monitoring purposes, it does not meet the stringent precision requirements for medical diagnosis and treatment decision-making, which necessitate adherence to international standards such as ISO 5725 [20] for measurement accuracy and precision. The current estimation performance requires significant improvement to achieve the metrological standards required for clinical diagnostic applications.

Future work requires multi-subject dataset validation, development of individually adaptive models, edge computing-compatible lightweight implementation, accuracy improvement through component-specific weighting, and technical improvements toward achieving medical diagnostic-level precision.

V. Conclusion

This fundamental study established and validated a three-dimensional knee contact force estimation system using wearable IMU sensors for knee osteoarthritis prevention. Through systematic comparison of four deep learning models, we identified optimal architectures for continuous healthcare monitoring applications. The 1D-CNN model achieved the best maximum error performance of 24.01 % NRMSE, while LSTM demonstrated superior average accuracy of 13.93 % NRMSE. These results outperformed existing IMU-based methods and fall within the practical accuracy range for wearable healthcare devices. The fundamental study established the technical feasibility of translating laboratory-based knee joint load assessment to daily environments. By extending conventional one-dimensional estimation to complete three-dimensional force estimation, this work provides a foundation for developing non-invasive knee osteoarthritis prevention systems that enable early intervention and personalized healthcare management in aging societies.

References

[1] "Global, regional prevalence, incidence and risk factors of knee osteoarthritis in population-based studies," ResearchGate. Accessed: Mar. 12, 2025. [Online]. Available: https://www.researchgate.net/publication/347242559_Global_regional_prevalence_incidence_and_risk_factors_of_knee_osteoarthritis_in_population-based_studies

[2] C. M. McDonough and A. M. Jette, "The contribution of osteoarthritis to functional limitations and disability," *Clin. Geriatr. Med.*, vol. 26, no. 3, pp. 387–399, Aug. 2010, doi: 10.1016/j.cger.2010.04.001.

[3] A. Shane Anderson and R. F. Loeser, "Why is osteoarthritis an age-related disease?," *Best Pract. Res. Clin. Rheumatol.*, vol. 24, no. 1, pp. 15–26, Feb. 2010, doi: 10.1016/j.berh.2009.08.006.

[4] D. T. Felson, "Osteoarthritis as a disease of mechanics," *Osteoarthritis Cartilage*, vol. 21, no. 1, pp. 10–15, Jan. 2013, doi: 10.1016/j.joca.2012.09.012.

[5] M. A. Verstraete, P. A. Meere, G. Salvadore, J. Victor, and P. S. Walker, "Contact forces in the tibiofemoral joint from soft tissue tensions: Implications to soft tissue balancing in total knee arthroplasty," *J. Biomech.*, vol. 58, pp. 195–202, Jun. 2017, doi: 10.1016/j.jbiomech.2017.05.008.

[6] K. R. Kaufman, N. Kovacevic, S. E. Irby, and C. W. Colwell, "Instrumented implant for measuring tibiofemoral forces," *J. Biomech.*, vol. 29, no. 5, pp. 667–671, May 1996, doi: 10.1016/0021-9290(95)00124-7.

[7] S. L. Delp *et al.*, "OpenSim: Open-Source Software to Create and Analyze Dynamic Simulations of Movement," *IEEE Trans. Biomed. Eng.*, vol. 54, no. 11, pp. 1940–1950, Jan. 2007, doi: 10.1109/TBME.2007.901024.

[8] J. Rasmussen, M. Damsgaard, E. Surma, S. Christensen, M. D. Zee, and V. Vondrák, "AnyBody - a software system for ergonomic optimization," 2003. Accessed: Mar. 29, 2025. [Online]. Available: https://www.semanticscholar.org/paper/AnyBody-a-software-system-for-ergonomic-Rasmussen-Damsgaard/22da7653c03cb4d505fd146421b95df2c4f86a49?p2df

[9] R. D. Gurchiek, R. S. McGinnis, A. R. Needle, J. M. McBride, and H. van Werkhoven, "The use of a single inertial sensor to estimate 3-dimensional ground reaction force during accelerative running tasks," *J. Biomech.*, vol. 61, pp. 263–268, Aug. 2017, doi: 10.1016/j.jbiomech.2017.07.035.

[10] T. Seel, J. Raisch, and T. Schauer, "IMU-Based Joint Angle Measurement for Gait Analysis," *Sensors*, vol. 14, no. 4, Art. no. 4, Apr. 2014, doi: 10.3390/s140406891.

[11] A. R. Zangene, R. A. Azar, H. Naserpour, and S. H. H. Nasab, "IMU-Based Estimation of the Knee Contact Force using Artificial Neural Networks," in *2022 29th National and 7th International Iranian Conference on Biomedical Engineering (ICBME)*, Feb. 2022, pp. 81–86. doi: 10.1109/ICBME57741.2022.10052800.

[12] T. Kuwahara, K. Hiroaki, and Y. Sankai, "IMU Sensor Module for the Measurement of High-speed Motion in the Analysis of Human Skills," presented at the proceedings of the International Symposium on System Integration (SII2019), Paris, France, 2019, pp. 560–565.

[13] R. B. Davis, S. Õunpuu, D. Tyburski, and J. R. Gage, "A gait analysis data collection and reduction technique," *Hum. Mov. Sci.*, vol. 10, no. 5, pp. 575–587, Oct. 1991, doi: 10.1016/0167-9457(91)90046-Z.

[14] D. S. Catelli, Wesseling ,Mariska, Jonkers ,Ilse, and M. and Lamontagne, "A musculoskeletal model customized for squatting task," *Comput. Methods Biomech. Biomed. Engin.*, vol. 22, no. 1, pp. 21–24, Jan. 2019, doi: 10.1080/10255842.2018.1523396.

[15] Y. Lecun, L. Bottou, Y. Bengio, and P. Haffner, "Gradient-based learning applied to document recognition," *Proc. IEEE*, vol. 86, no. 11, pp. 2278–2324, Jan. 1998, doi: 10.1109/5.726791.

[16] W. Tang, G. Long, L. Liu, T. Zhou, M. Blumenstein, and J. Jiang, "Omni-Scale CNNs: a simple and effective kernel size configuration for time series classification," Jun. 17, 2022, *arXiv*: arXiv:2002.10061. doi: 10.48550/arXiv.2002.10061.

[17] S. Hochreiter and J. Schmidhuber, "Long Short-Term Memory," *Neural Comput.*, vol. 9, no. 8, pp. 1735–1780, Jan. 1997, doi: 10.1162/neco.1997.9.8.1735.

[18] J. L. Elman, "Finding Structure in Time," *Cogn. Sci.*, vol. 14, no. 2, pp. 179–211, 1990, doi: 10.1207/s15516709cog1402_1.

[19] A. Vaswani *et al.*, "Attention Is All You Need," Aug. 02, 2023, *arXiv*: arXiv:1706.03762. doi: 10.48550/arXiv.1706.03762.

[20] "ISO 5725-1:2023(en), Accuracy (trueness and precision) of measurement methods and results — Part 1: General principles and definitions." Accessed: Aug. 31, 2025. [Online]. Available: https://www.iso.org/obp/ui/#iso:std:iso:5725:-1:ed-2:v1:en